Leibniz Gemeinschaft

WIAS

Weierstrass Institute for Applied Analysis and Stochastics

in Forschungsverbund Berlin e.V., Mohrenstrasse 39, D - 10117 Berlin, Germany

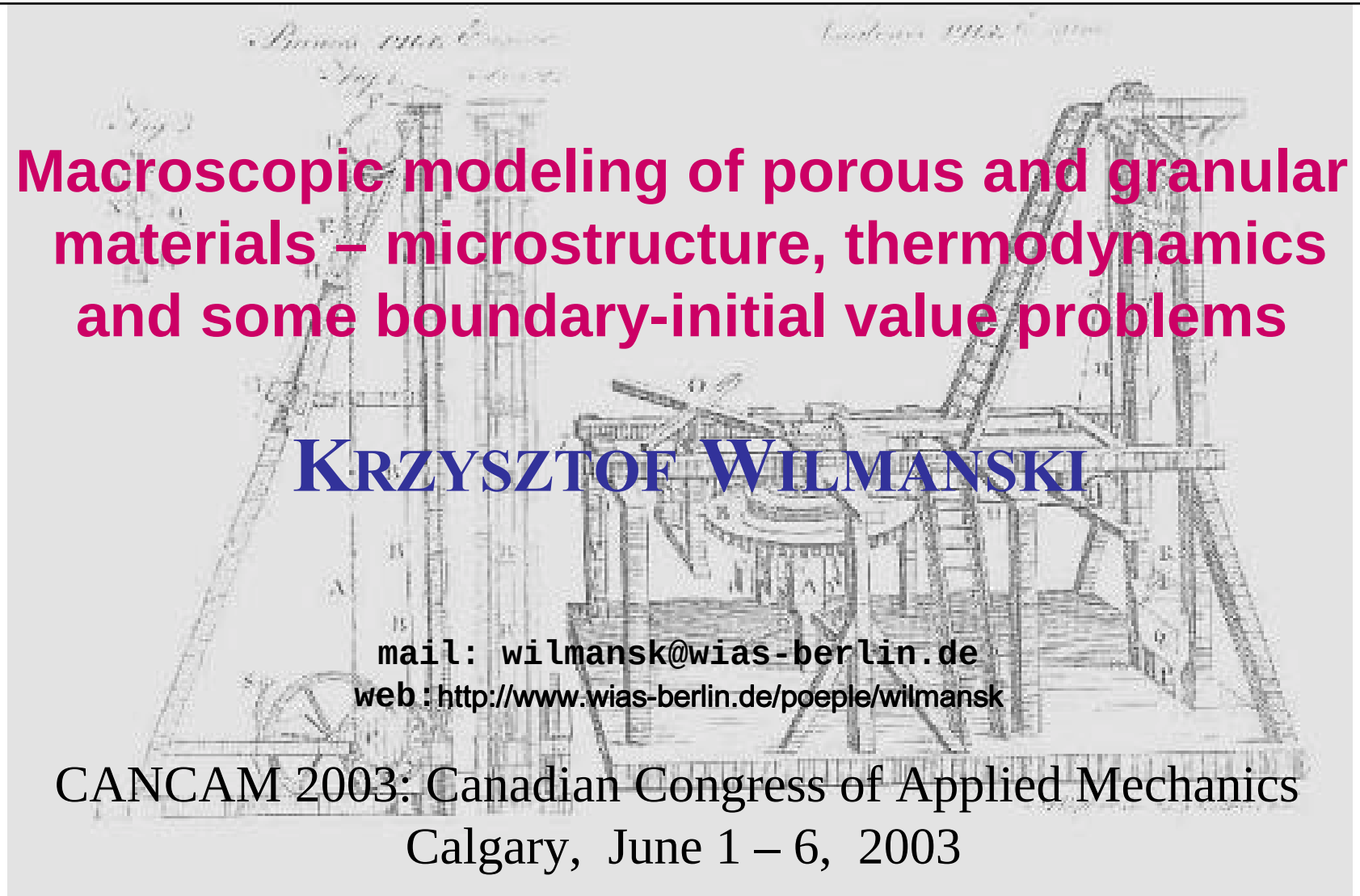

Macroscopic modeling of porous and granular materials – microstructure, thermodynamics and some boundary-initial value problems

KRZYSZTOF WILMANSKI

mail: wilmansk@wias-berlin.de

web : http://www.wias-berlin.de/poeple/wilmansk

CANCAM 2003: Canadian Congress of Applied Mechanics

Calgary, June 1 – 6, 2003

Pile boring machines of the 18th century

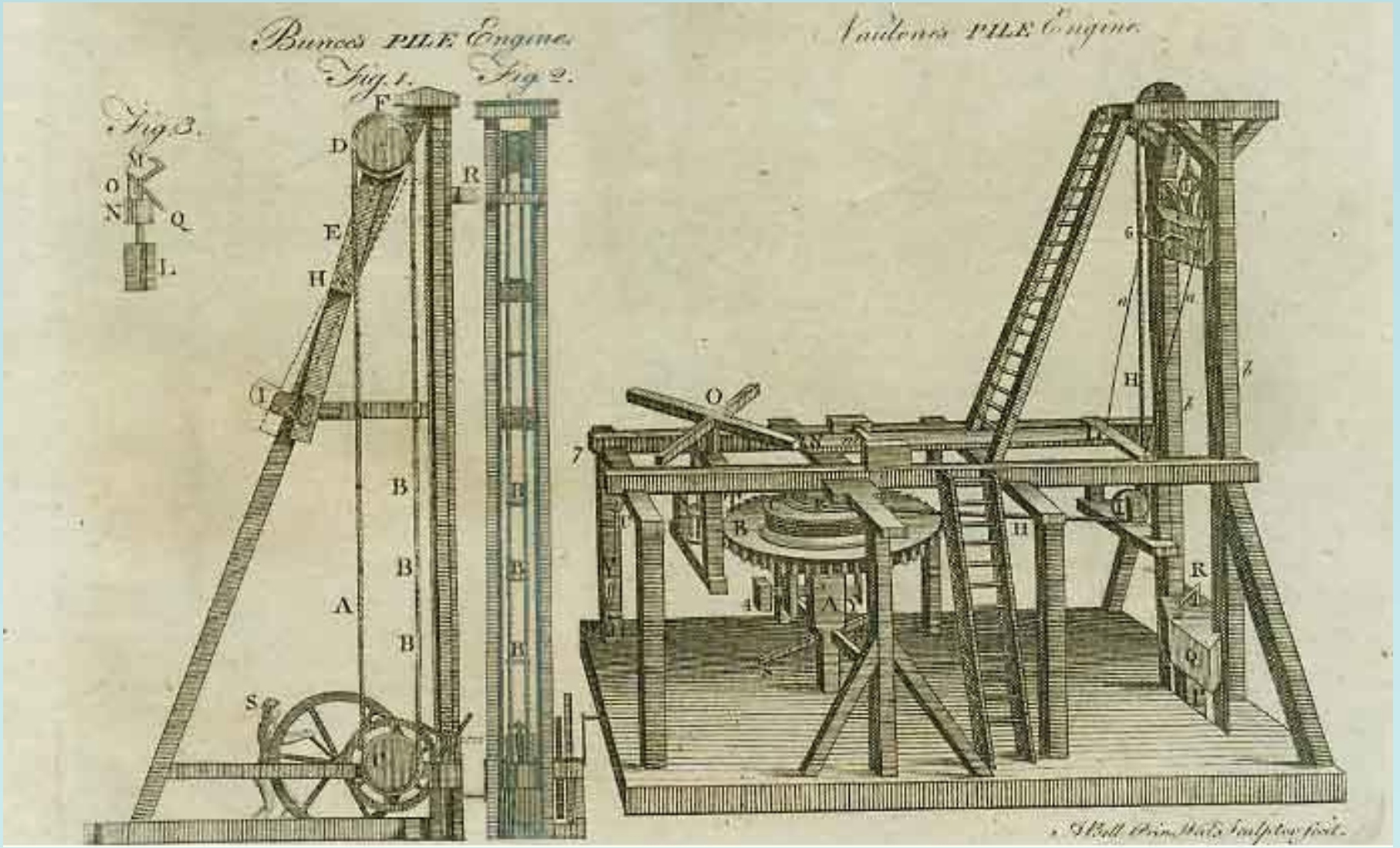

„Bunces Pile Engine“ *„Vaulone‘s Pile Engine “*

Taken from the *Encyclopedia Britanica*, 1797-1803 by D. P. Zeccos

Liquefaction (piping) of saturated soils

Landslide in El Salvador (Colonia Las Colinas) *by the earthquake* 13.01.2001

Most important microstructural parameters for design and forecast: porosity, saturation, permeability, confining pressure

Tilt due to liquefaction
(Adapazari)

Liquefaction (Monterey)

Ground rupture (Taiwan)

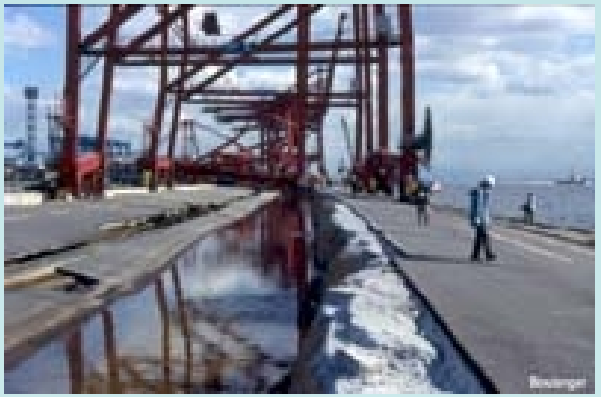

Liquefaction (Kobe)

Tilt due to liquefaction
(Kobe)

Contents:

1. Microstructure

- solid component (skeleton, granuli, platelets, etc.) and fluid components (liquid or liquids and gases and/or vapours), mass exchange between components (chemical reactions, evaporation/condensation, freezing/melting, adsorption),
- different kinematics of components – diffusion,
- „static“ interactions: bindings, changes of porosity, local fluctuations of kinetic energies – tortuosity.

2. Multicomponent continuous models

- immiscible mixture,
- Biot/Terzaghi/Darcy.

3. Thermodynamics

- entropy inequality and its evaluation, dissipation,
- differential equations for porosity, stresses (plastic deformations, non-Newtonian fluid components, adsorption and chemical reactions),
- some open problems, e.g. multiple temperatures

4. Some boundary – initial value problems

Microstructure:

Pore casts (epoxy replicas, Bourbié)

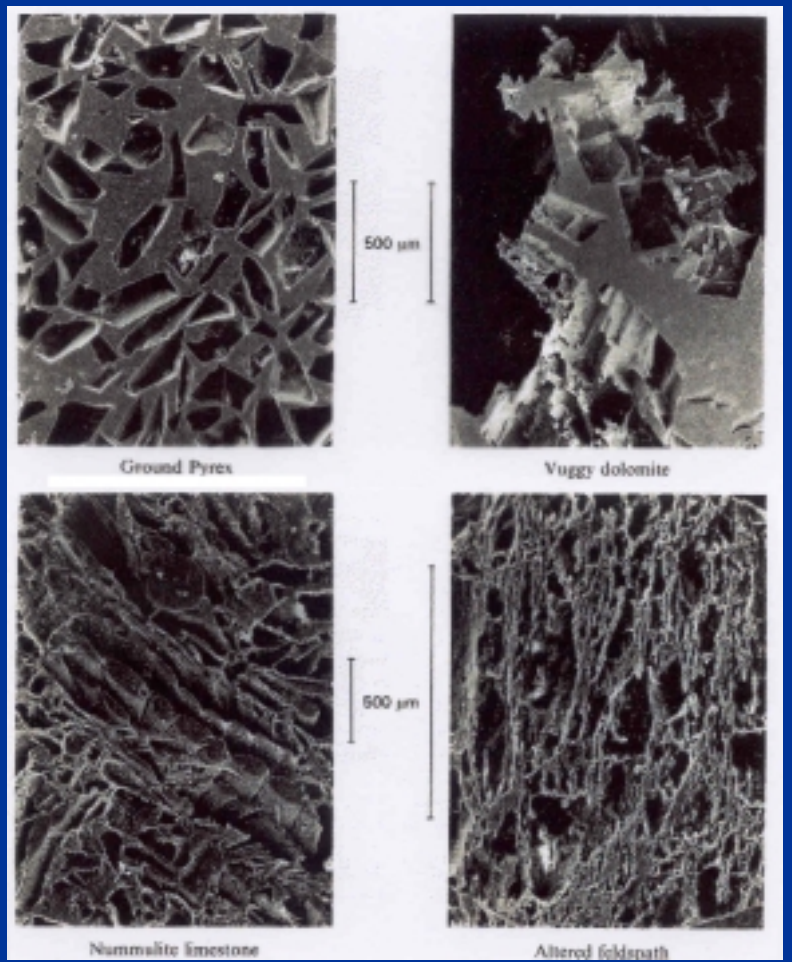

Sandstone in diagenesis

Microstructure:

(after: T. Bourbie, O. Coussy, B. Zinszner; *Acoustics of Porous Media*, 1987.

VISUALIZATION OF CAPILLARY PROPERTIES

Photographs of thin sections of rocks selectively saturated with dyed resins or Wood's metal by drainage and imbibition

Photo 1 — *Total imbibition*. Vuggy dolomite (dolomitized oolitic limestone). Red resin, wetting fluid. Yellow resin, residual non-wetting fluid (trapped). The characteristic shape ("bubbles") of the clusters of residual non-wetting fluid can be observed.

Photo 2 — *Drainage and imbibition*. Crinoidal limestone. The sample, first saturated with blue resin, was centrifuged to irreducible saturation, and then, after polymerization of the blue resin, impregnated with red resin. Blue resin represents irreducible wetting fluid. Red resin represents the fraction displaceable by imbibition of the non-wetting fluid accumulated during drainage. Yellow resin represents the residual fraction of non-wetting fluid. Note particularly a petrographic detail which plays an important role in the distribution of the displaceable and trapped phases of the non-wetting fluid. The fine layer of palisadic cement surrounding the crinoids has burst under the effect of compaction, and the fragments of cement part the intergranular spaces, favoring imbibition (red resin) without substantially altering the rock structure. The pore spaces devoid of these fragments usually correspond to trapped porosity (yellow resin). This compartmentation process, which reduces trapped porosity, is not an exceptional occurrence.

Photo 3 — *Drainage*. Ground Pyrex. Molten Wood's metal behaves like mercury (non-wetting fluid) and porosimetry experiments can be performed in which this metal is frozen by cooling. Black, Wood's metal (drained zones). Red resin, subsequently injected (undrained zones).

Photo 4 — *Successive drainages*. Crinoidal limestone. The rock, first saturated with blue resin, was subjected to drainage by centrifuge, and then, after polymerization, to saturation with red resin, followed by centrifuge under low acceleration. It was then saturated with yellow resin. The color of the resin present in a pore depends on the access radius.

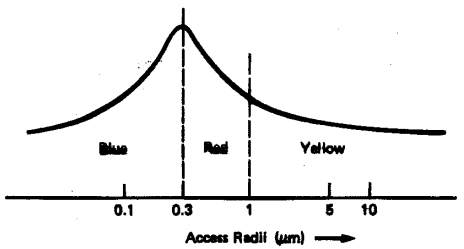

The very small access radius zones (blue resin) correspond to microporosity in the crinoids (invisible in transmitted light) and also to intragranular macroporosity. A good intergranular porosity (red resin) is connected by flow channels smaller than 1 μm. This is frequently encountered in well-cemented bioclastic grainstones.

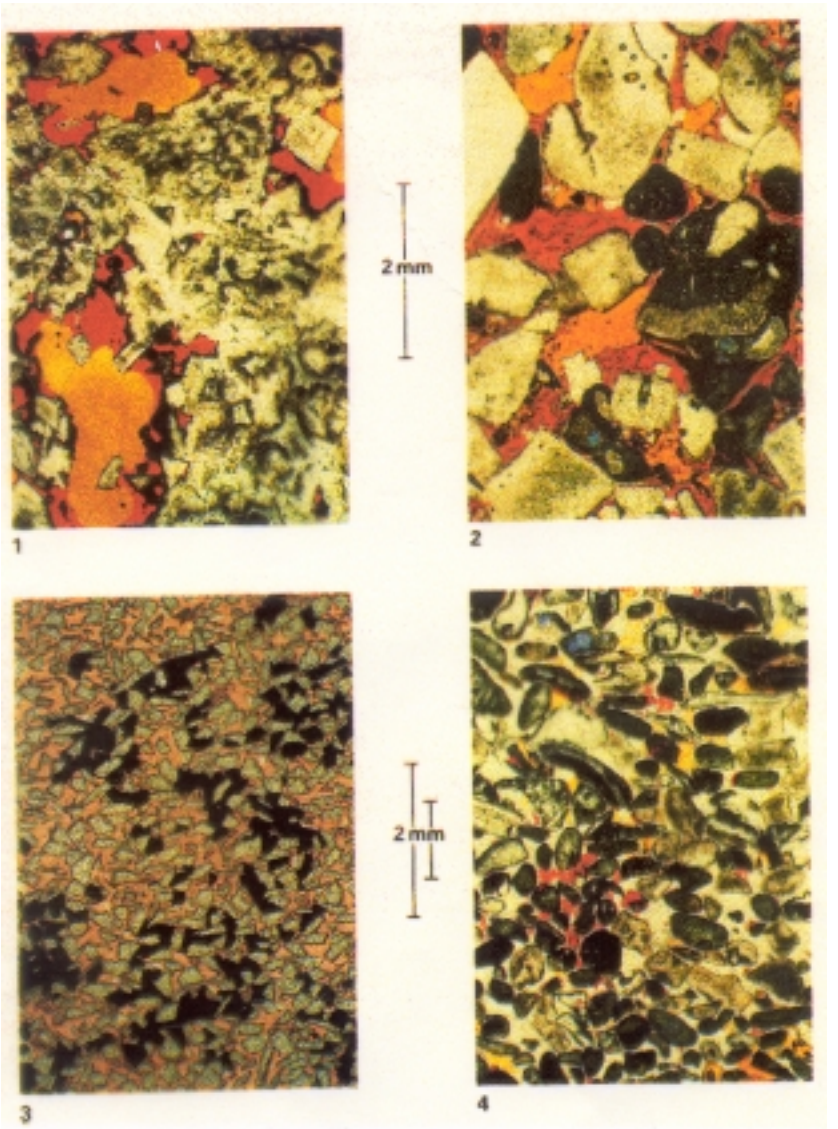

Microstructure:

Toilet paper

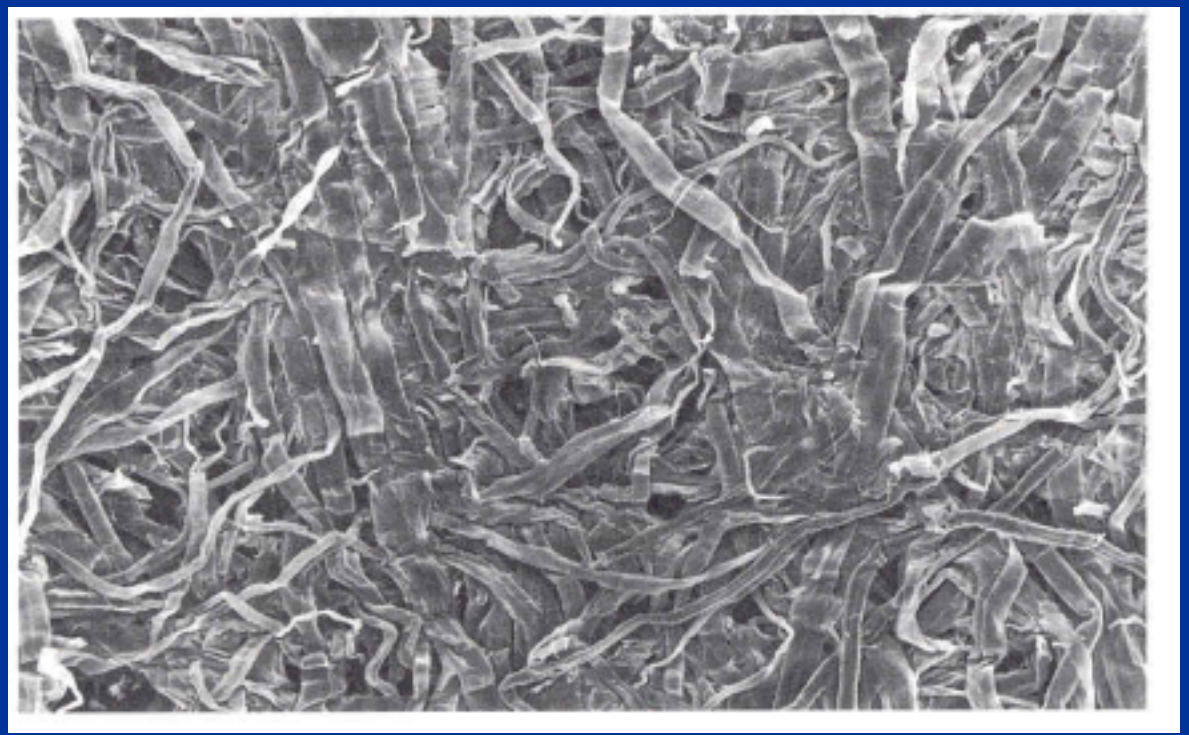

Oscillon

Paul Umbanhowar (Northwestern Univ.)

icrostructure:

Biomechanics:
Lungs

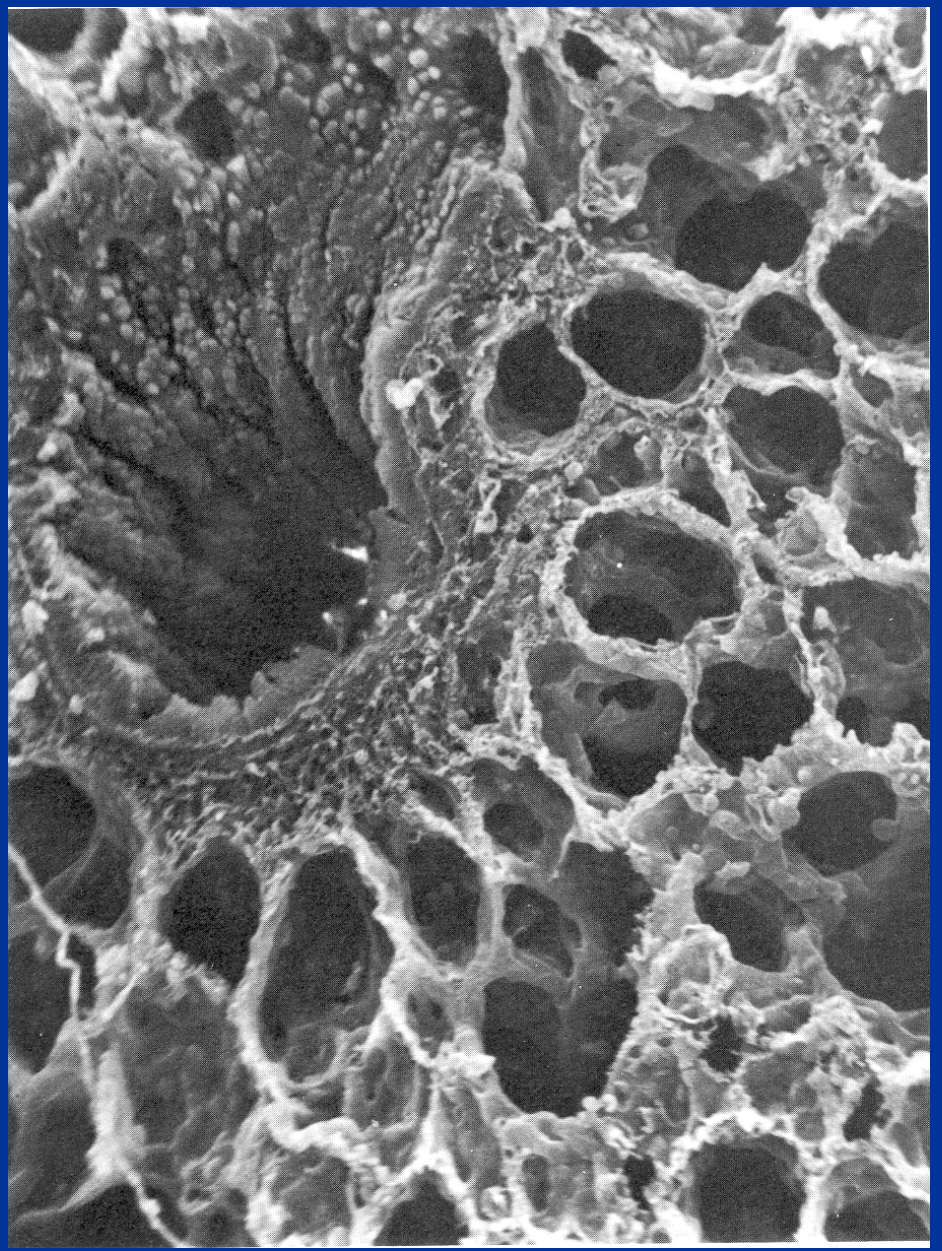

ulticomponent continuous models:

1. Microscopic description

a. fields $u^R \in \Re^n$:

ρ^{SR} - true (real) mass density of the skeleton,

$\rho^{\alpha R}$ - true (real) mass densities of fluid components, $\alpha=1,\ldots,A$,

$\mathbf{v}^{SR}$ - true velocity of the skeleton,

$\mathbf{v}^{\alpha R}$ - true velocities of fluid components,

θ^{SR} - temperature of the skeleton,

$\theta^{\alpha R}$ - temperatures of fluid components,

ν^{mR}, $m=1,\ldots,M$, - internal variables (extents of chemical reactions, phase fractions, real plastic deformations, etc.).

b. balance laws

mass, momentum, energy.

c. constitutive laws

stress – strain relations, evolution equations, etc.

d. microscopic field equations (in the form of a set of first order equations)

$$\frac{\partial}{\partial t}\mathbf{F}^{0R}(\mathbf{u}^R)+\frac{\partial}{\partial x^k}\mathbf{F}^{kR}(\mathbf{u}^R)=\hat{\mathbf{F}}^R(\mathbf{u}^R).$$

Due to geometrical complexity solutions are impossible!

ulticomponent continuous models:

2. Micro-macrotransition

- kinetic theories, Boltzmann-like equations for distribution function – applicable for granular gases (Saturn rings, etc.)

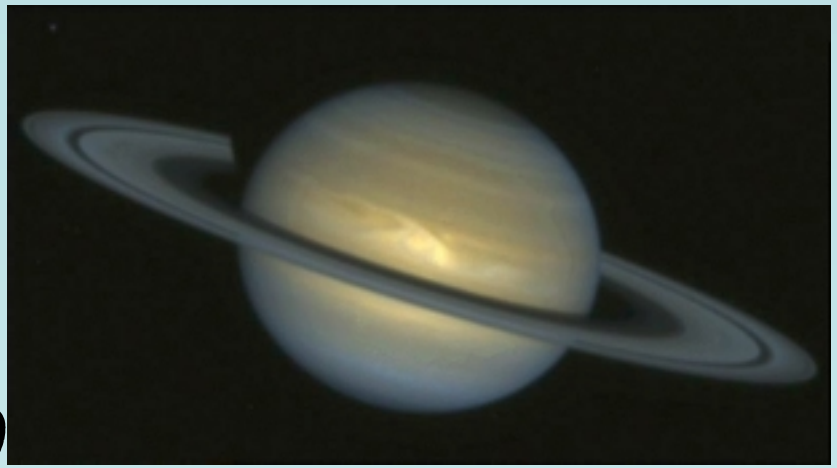

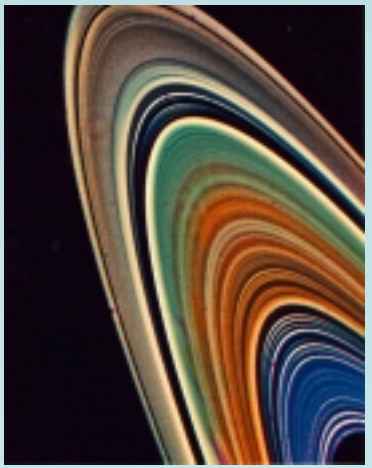

- volume averaging, representative elementary volume (REV)

$$\rho_t^S(\mathbf{x},t)=\frac{1}{V(REV)}\int_{REV(\mathbf{x})}\rho^{SR}(\mathbf{z},t)H^S(\mathbf{z},t)dV_{\mathbf{z}},$$

$$\rho_t^\alpha(\mathbf{x},t)=\frac{1}{V(REV)}\int_{REV(\mathbf{x})}\rho^{\alpha R}(\mathbf{z},t)H^\alpha(\mathbf{z},t)dV_{\mathbf{z}},$$

and similarly for other fields.

important particular case – homogeneous microstructure $\Rightarrow_{12}$

$\Rightarrow$ Gassmann relations (see: later!)

Two-component macroscopic isothermal model of saturated porous materials*: fields (linear)

Micro-macro:

$$\rho_t^S = (1-n)\rho^{SR}, \quad \rho_t^F = n\rho^{FR},$$

$$\rho_t^S = \frac{\rho_0^S}{1+e}, \quad \rho_t^F = \frac{\rho_0^F}{1+\varepsilon},$$

$$\rho_t^{SR} = \frac{\rho_0^{SR}}{1+e^R}, \quad \rho_t^{FR} = \frac{\rho_0^{FR}}{1+\varepsilon^R},$$

$e, \varepsilon, e^R, \varepsilon^R$ - volume changes

Geometrical compatibility (linear):

$$e = e^R + \frac{n-n_0}{1-n_0},$$

$$\varepsilon = \varepsilon^R - \frac{n-n_0}{n_0}.$$

$\rho^S{}_t$ – current partial mass density of the skeleton,

$\rho^F{}_t$ – current partial mass density of the fluid,

$\mathbf{v}^S$ – current partial velocity of the skeleton,

$\mathbf{e}^S$ – Almansi Hamel deformation tensor

$\mathbf{v}^F$ – current partial velocity of the fluid,

n – current porosity, n_E – equilibrium porosity.

fluxes

$\mathbf{T}^S$ – partial Cauchy stress tensor in the skeleton,

$\mathbf{T}^F$ – partial Cauchy stress tensor in the fluid.

*Biot, M; since 1941, linear model. see: I. Tolstoy (ed.), *Twenty-one Papers by M. A. Biot*, Am. Inst. Physics, (1990),
Wilmanski, K.; *Thermomechanics of Continua,* Springer, Berlin (1998).

Partial balance equations:

Mass balance:

$$\frac{\partial \rho_t^S}{\partial t} + div\left(\rho_t^S \mathbf{v}^S\right) = \hat{\rho}^S, \quad \frac{\partial \rho_t^F}{\partial t} + div\left(\rho_t^F \mathbf{v}^F\right) = -\hat{\rho}^S,$$

Momentum balance:

$$\frac{\partial \rho_t^S \mathbf{v}^S}{\partial t} + div\left(\rho_t^S \mathbf{v}^S \otimes \mathbf{v}^S - \mathbf{T}^S\right) = \hat{\mathbf{p}},$$

$$\frac{\partial \rho_t^F \mathbf{v}^F}{\partial t} + div\left(\rho_t^F \mathbf{v}^F \otimes \mathbf{v}^F - \mathbf{T}^F\right) = -\hat{\mathbf{p}},$$

Porosity balance:

$$\frac{\partial n J^{S-1}}{\partial t} + div\left[n\mathbf{v}^S + \Phi(n_E)\left(\mathbf{v}^F - \mathbf{v}^S\right)\right] = \left(\hat{n} + \delta \frac{\partial J^S}{\partial t}\right) J^{S-1}, \quad J^S := 1 + tr\,\mathbf{e}^S \equiv 1 + e.$$

Integrability (linear – existence of displacement):

$$\frac{\partial \mathbf{e}^S}{\partial t} = grad\,\mathbf{v}^S \quad \Rightarrow \quad \exists \mathbf{u}^S : \mathbf{v}^S = \frac{\partial \mathbf{u}^S}{\partial t}, \mathbf{e}^S = sym\,grad\,\mathbf{u}^S.$$

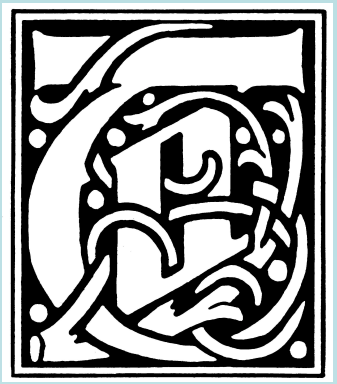

hermodynamics:

1) Constitutive assumptions for

$$\hat{\rho}^S, \mathbf{T}^S, \mathbf{T}^F, \hat{\mathbf{p}}, \Phi, \hat{n} \quad \Rightarrow$$

2) Field equations for fundamental fields

3) Thermodynamic admissibility:
for all solutions of field equations the entropy inequality

$$\frac{\partial}{\partial t}(\rho_t^S \eta^S + \rho_t^F \eta^F) + div(\rho_t^S \eta^S \mathbf{v}^S + \rho_t^F \eta^F \mathbf{v}^F + \mathbf{h}^S + \mathbf{h}^F) \geq 0,$$

must be satisfied identically.

In this inequaliy η^S, η^F are partial entropy functions,
and $\mathbf{h}^S$, $\mathbf{h}^F$ - their fluxes, all given by constitutive relations.

Thermodynamics:

Results from the evaluation of the entropy inequality:
- **identities relating constitutive equations of various quantities; Gibbs equations, thermodynamic potentials,**
- **dissipation inequality defining the state of thermodynamic equilibrium and restricting mechanisms of dissipation.**

Dissipation inequality for isothermal procresses in two-component linear poroelastic material:

$$\mathsf{D} := (\mu^S - \mu^F)\hat{\rho}^S + \hat{\mathbf{p}} \cdot (\mathbf{v}^F - \mathbf{v}^S) + \frac{\partial}{\partial n}(\rho^S \psi^S + \rho^F \psi^F)\hat{n} \geq 0,$$

where μ^S, μ^F are chemical potentials of both components, ψ^S, ψ^F are their Helmholtz free energies.

The state of thermodynamic equilibrium:

$$\mu^S = \mu^F, \quad \mathbf{v}^S = \mathbf{v}^F, \quad \hat{n} = 0,$$

i.e. - no mass exchange,
- no diffusion,
- no porosity relaxation.

Most models are based on the assumption of linear deviation from the thermodynamic equilibrium!

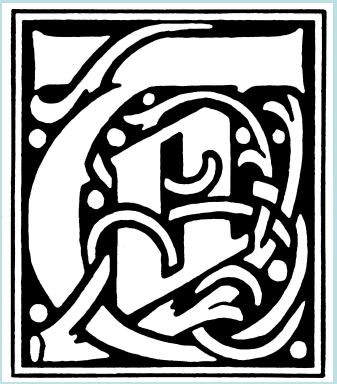

hermodynamics:

Some examples of generalizations:

1) Hypoplastic materials – modeling of soils, evolution equation for effective stresses in the skeleton (Terzaghi – Kolymbas),
2) Langmuir model of adsorption – mass exchange by settlement of pollutants,
3) Drying of wood – evaporation (phase transformation) processes,
4) Freezing – phase transformation with a free surface.

Constitutive relations for poroelastic materials

Assumption: linear elasticity, ideal fluid

Partial stress tensors:

BIOT

POROSITY GRADIENT

$$\mathbf{T}^S = \mathbf{T}_0^S + \lambda^S e\mathbf{1} + 2\mu^S \mathbf{e}^S + Q\varepsilon\mathbf{1} - N(n-n_0)\mathbf{1} + \beta(n-n_E)\mathbf{1}, \quad e := tr\,\mathbf{e}^S,$$

$$\mathbf{T}^F = -\left[p_0^F - \rho_0^F \kappa\varepsilon + Qe - N(n-n_0) + \beta(n-n_E)\right]\mathbf{1}, \quad \varepsilon := -\frac{\rho^F - \rho_0^F}{\rho_0^F}$$

nonequilibrium contribution

Sources

$$\hat{\mathbf{p}} = \pi(\mathbf{v}^F - \mathbf{v}^S), \quad \hat{n} = -\frac{n-n_E}{\tau}.$$

relaxation time

Porosity

$$= 1 + e - \varepsilon$$

$$n = n_0\left[1 + \gamma\left(\frac{\rho^F}{\rho_0^F}\frac{\rho_0^S}{\rho^S} - 1\right)\right] + \delta\, n_0 e - n_0 \frac{\gamma}{\tau}\int_0^t (e-\varepsilon)_{t-s}\, e^{-\frac{s}{\tau}} ds.$$

Bulk stress and pore pressure of soil mechanics

$$\mathbf{T} := \mathbf{T}^S + \mathbf{T}^F = \mathbf{T}_0 + (K - \frac{2}{3}\mu^S)e\mathbf{1} + 2\mu^S \mathbf{e}^S - C\zeta\mathbf{1}, \quad \zeta := n_0(e - \varepsilon),$$

$$\mathbf{T}^F = -n_0 p_f, \quad p_f = p_f^0 - Ce + M\zeta - N\frac{n - n_0}{n_0},$$

increment of fluid content

Notation

$$K := \lambda^S + \frac{2}{3}\mu^S + \rho_0^F \kappa + 2Q, \quad C := \frac{1}{n_0}(Q + \rho_0^F \kappa), \quad M := \frac{\rho_0^F \kappa}{n_0}.$$

Pressures: $p^S := -tr\,\mathbf{T}^S, \quad p^F := -tr\,\mathbf{T}^F,$

- partial

- bulk and pore pressure

$$p^S - p_0^S = -\left(\lambda^S + \frac{2}{3}\mu^S + Q\right)e + \frac{Q}{n_0}\zeta + N(n - n_0),$$

$$p^F - p_0^F = -\left(\rho_0^F \kappa + Q\right)e + \frac{Q}{n_0}\zeta - N(n - n_0),$$

$$p \equiv p^F + p^S = p_0 - Ke + C\zeta,$$

$$p_f \equiv \frac{1}{n_0}p^F = p_f^0 - Ce + M\zeta - N\frac{n - n_0}{n_0}.$$

Micro-macrotransitions: Gedankenexperiments (elementary tests)

Mechanical equilibrium: $p = p_0 + \Delta p.$

jacketed

a) unjacketed

b) undrained

c) drained

$$p^F - p_0^F = n_0 \, \Delta p$$

$$\frac{d\rho^F V}{dt} = 0 \quad i.e. \quad \zeta = 0,$$

$$p^F - p_0^F = 0 \quad i.e.$$

$$p_f - p_f^0 = 0,$$

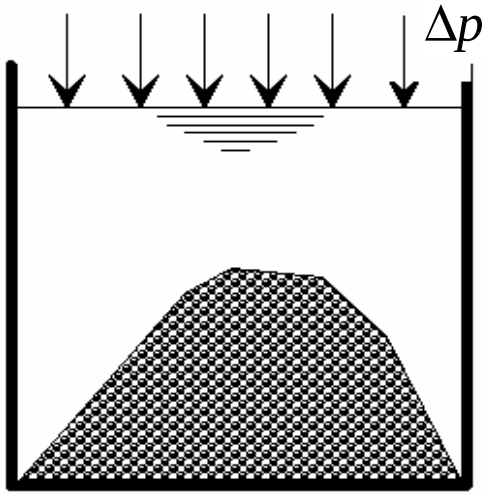

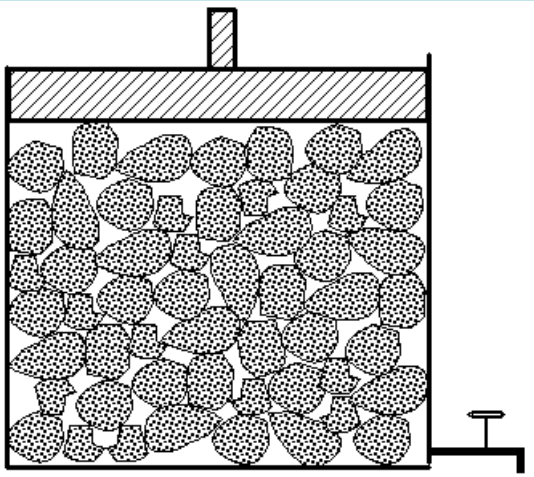

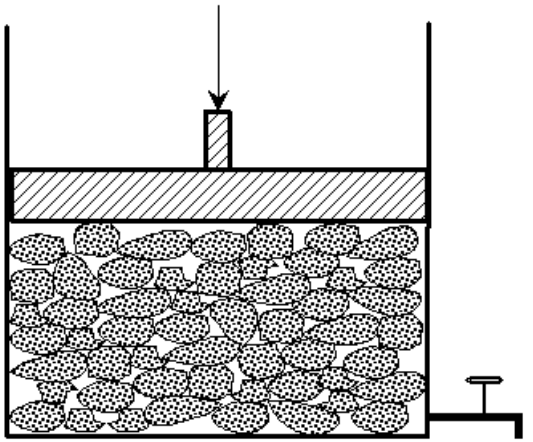

Microscopic constitutive relations

$$p^{SR} - p_0^{SR} = -K_s e^R, \quad p^{FR} - p_0^{FR} = -K_f \varepsilon^R.$$

Results of Gedankenexperiments - Gassmann relations $N \approx 0$

$$K = \frac{(K_s - K_f)^2}{\frac{K_s^2}{K_W} - K_b} + K_b, \quad C = \frac{K_s(K_s - K_b)}{\frac{K_s^2}{K_W} - K_b}, \quad M = \frac{K_s^2}{\frac{K_s^2}{K_W} - K_b},$$

where

$$\frac{1}{K_W} := \frac{1-n_0}{K_s} + \frac{n_0}{K_f},$$

and K_s, K_f, K_b are given from laboratory experiments, the latter – drained modulus.

These relations give a dependence of macroscopic parameters on the porosity n_0 .
Inverse problem: porosity from measurements of bulk and surface waves!

Numerical example*

$$K_s := 48.2\times10^9\,Pa, \quad K_f := 3.3\times10^9\,Pa.$$

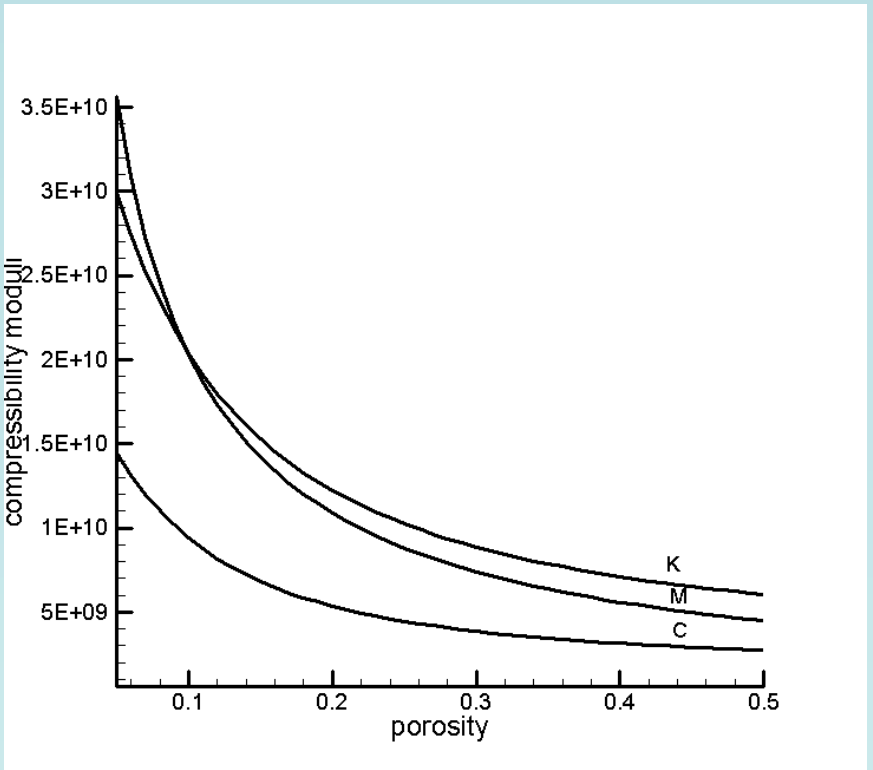

Macroscopic material parameters K, C, M

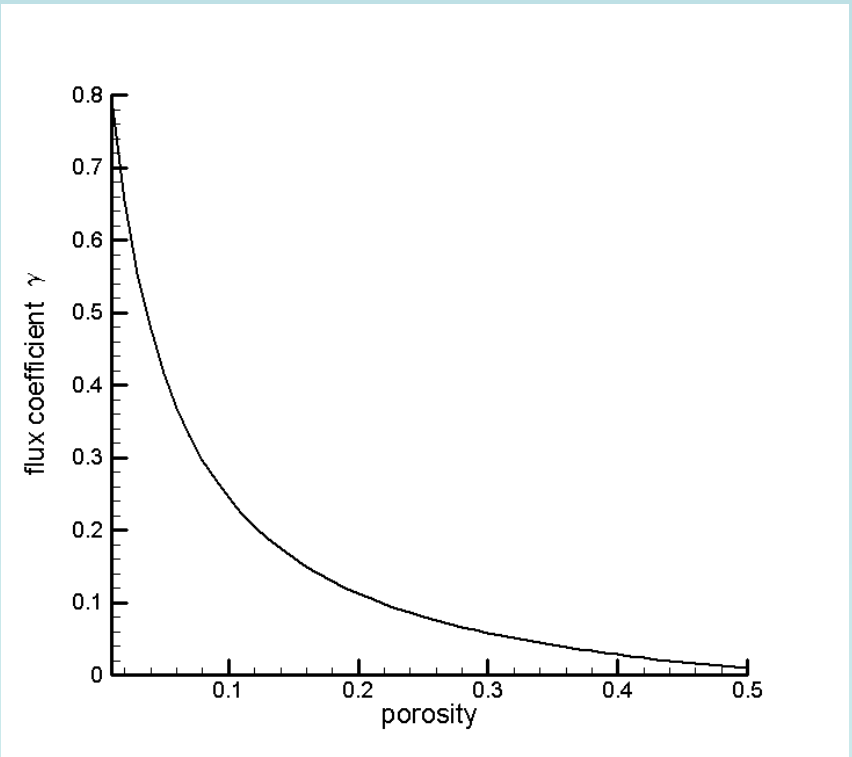

Porosity parameter γ

* The data are taken from: A.H.-D. Cheng; *Material coefficients of anisotropic poroelasticity, Int. J. Rock Mech. Min. Sci..,* **34**, 2, 199-205 (1997).

And fetch shrill echoes from the hollow earth
(**Shakespeare**, The Tempest, Act 5, Scene 1)

ome boundary – initial value problems:

Waves:

1. Propagation of linear bulk sound waves, their applications in nondestructive testing of soils, tissues, etc., noise control,
2. Surface waves in soils: earthquakes, nondestructive testing,
3. Nonlinear waves (shocks, solitons) near centers of explosions and earthquake‘s epicenters; medical applications of shock waves.

Instabilities:

1. Liquefaction of sands due to interactions with waves,
2. Landslides and avalanches,
3. Piping due to fast flows of fluids through granular materials,
4. Flow instabilities due to mass exchange.

Some boundary – initial value problems: waves

Dr. Dan Russel, Kettering University Applied Physics

http://www.kettering.edu/~drussell/Demos/reflect/reflect.html

Longitudinal wave

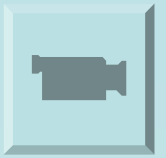

Transversal wave

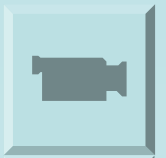

Mexican wave

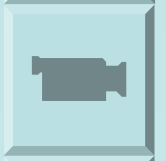

Water wave

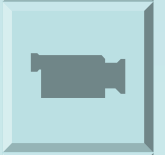

Rayleigh wave

Some boundary – initial value problems: waves

Influence of boundary condition on transmission and reflexion - impedance

Dr. **Dan Russel**, Kettering University, Applied Physics

http://www.kettering.edu/~drussell/Demos/reflect/reflect.html

at a fixed (hard) boundary, the displacement remains zero (Dirichlet conditions) and the reflected wave changes its polarity (undergoes a 180^0 phase change)

hard.gif

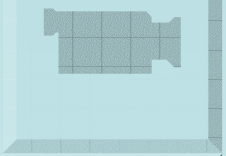

at a free (soft) boundary, the restoring force is zero (Neumann conditions) and the reflected wave has the same polarity (no phase change) as the incident wave

soft.gif

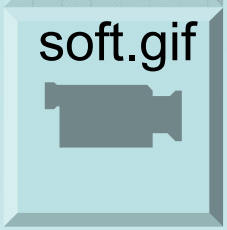

Permeable boundary: the incident wave is travelling from a region of low impedance towards a high impedance region

reflect1.gif

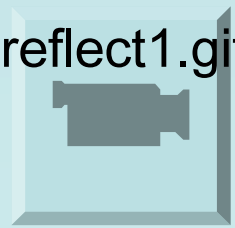

Permeable boundary: the incident wave is travelling from a high impedance region towards a low impedance region

reflect2.gif

Bulk monochromatic waves within the simple model: $Q = 0$

Ansatz:

$$\rho^F - \rho_0^F = R^F e^{i(k\mathbf{n}\cdot\mathbf{x}-\omega t)}, \quad \mathbf{e}^S = \mathbf{E}^S e^{i(k\mathbf{n}\cdot\mathbf{x}-\omega t)},$$

$$\mathbf{v}^F = \mathbf{V}^F e^{i(k\mathbf{n}\cdot\mathbf{x}-\omega t)}, \quad \mathbf{v}^S = \mathbf{V}^S e^{i(k\mathbf{n}\cdot\mathbf{x}-\omega t)},$$

$R^F, \mathbf{E}^S, \mathbf{V}^F, \mathbf{V}^S$ - constant amplitudes,

$\mathbf{n}, k, \omega$ - direction of propagation, wave number, and frequency.

Compatibility with field equations (ansatz: $\beta \approx 0$):

$$R^F = \frac{k\rho_0^F}{\omega}\mathbf{V}^F \cdot \mathbf{n}, \quad \mathbf{E}^S = -\frac{k}{2\omega}\left(\mathbf{V}^S \otimes \mathbf{n} + \mathbf{n} \otimes \mathbf{V}^S\right),$$

$$\left(\omega^2 \mathbf{1} - \frac{\lambda^S + \mu^S}{\rho_0^S}k^2 \mathbf{n}\otimes\mathbf{n} - \frac{\mu^S}{\rho_0^S}k^2\mathbf{1} + i\frac{\pi\omega}{\rho_0^S}\mathbf{1}\right)\mathbf{V}^S - i\frac{\pi\omega}{\rho_0^S}\mathbf{V}^F = 0,$$

$$-i\frac{\pi\omega}{\rho_0^F}\mathbf{V}^S + \left(\omega^2\mathbf{1} - \kappa k^2 \mathbf{n}\otimes\mathbf{n} + i\frac{\pi\omega}{\rho_0^F}\mathbf{1}\right)\mathbf{V}^F = 0.$$

Longitudinal waves: solution of the dispersion relation

$$k^2 = \frac{1}{2}\left[\frac{1}{c_{P1}^2}\left(\omega^2 + i\frac{\pi\omega}{\rho_0^S}\right) + \frac{1}{c_{P2}^2}\left(\omega^2 + i\frac{\pi\omega}{\rho_0^F}\right) \pm \sqrt{D}\right],$$

$$D := \left[\frac{1}{c_{P1}^2}\left(\omega^2 + i\frac{\pi\omega}{\rho_0^S}\right) - \frac{1}{c_{P2}^2}\left(\omega^2 + i\frac{\pi\omega}{\rho_0^F}\right)\right] - \frac{4}{c_{P1}^2 c_{P2}^2}\frac{\pi^2\omega^2}{\rho_0^S \rho_0^F}.$$

$$c_{P1}^2 := \frac{\lambda^S + 2\mu^S}{\rho_0^S},$$

$$c_{P2}^2 := \kappa.$$

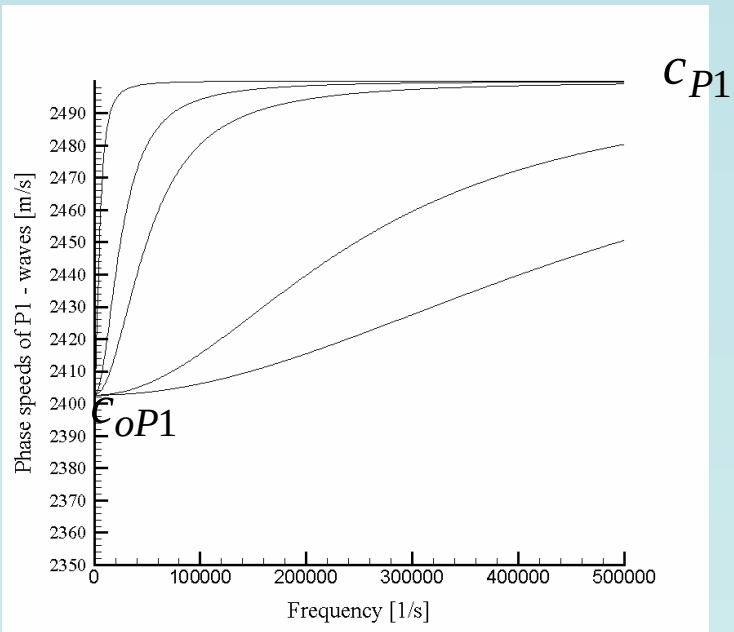

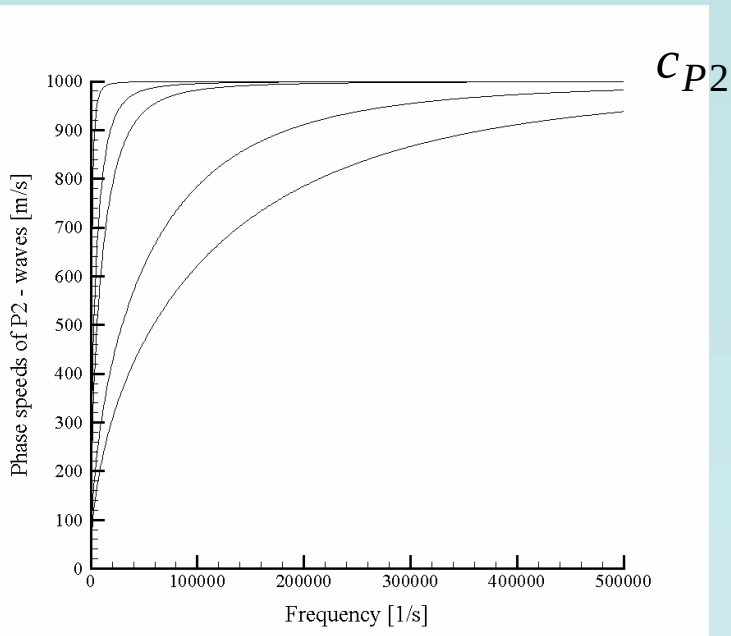

Phase speed ω/Rek of P1 and P2 – waves as functions of the frequency ω for c_{P1}=2500 m/s, c_{P2}=1000 m/s, ρ_0^S=2500 kg/m³, ρ_0^F =250 kg/m³, permeability coefficient: π =10⁶, 5×10⁶, 10⁷, 5×10⁷, 10⁸ kg/m³s.

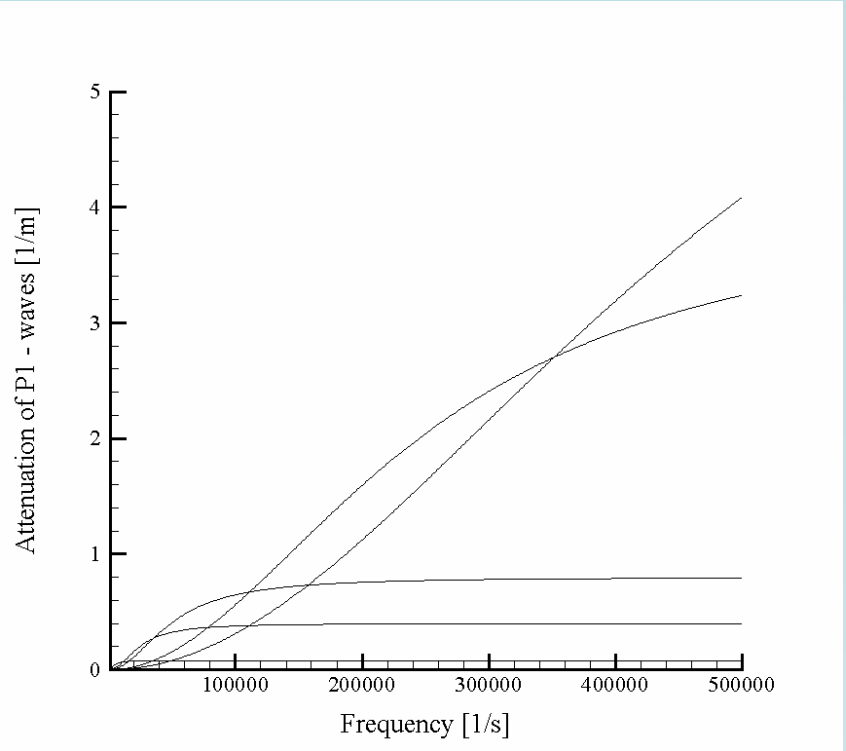

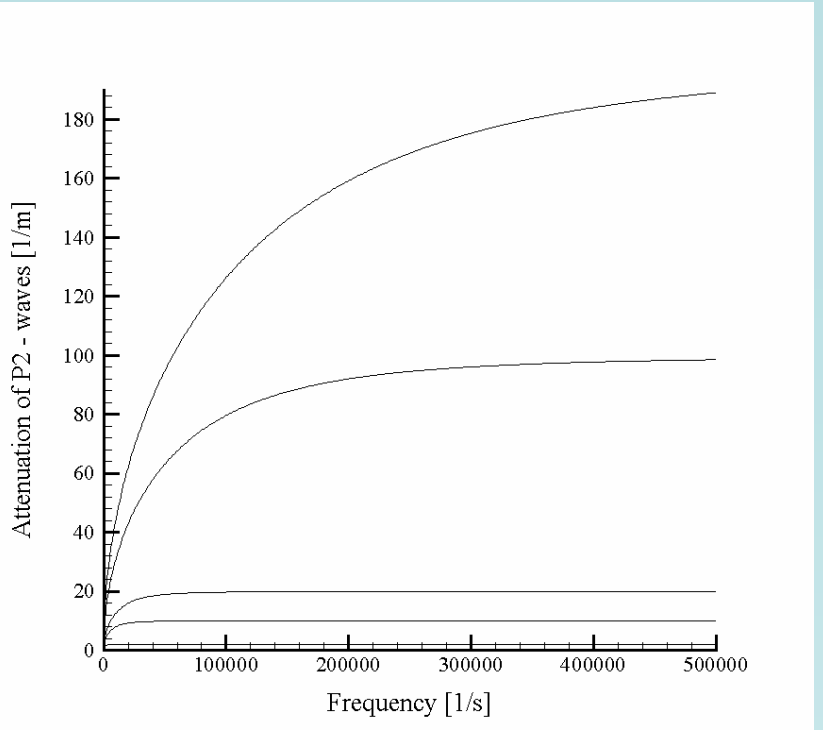

Attenuation Im*k* *of P1 and P2 – waves as functions of the frequency ω for* c_{P1} *=2500 m/s,* c_{P2} *=1000 m/s,* ρ_0^S *=2500 kg/m³,* ρ_0^F *=250 kg/m³, permeability coefficient:* $\pi = 10^6, 5\times10^6, 10^7, 5\times10^7, 10^8$ *kg/m³s.*

Limits:

$$P1: \quad c_{oP1} := \lim_{\omega\to 0}\frac{\omega}{\mathrm{Re}\,k} = \sqrt{\frac{\lambda^S + 2\mu^S + \kappa\rho_0^F}{\rho_0^S + \rho_0^F}}, \quad \lim_{\omega\to\infty}\frac{\omega}{\mathrm{Re}\,k} = c_{P1},$$

$$P2: \quad c_{oP2} := \lim_{\omega\to 0}\frac{\omega}{\mathrm{Re}\,k} = 0, \quad \lim_{\omega\to\infty}\frac{\omega}{\mathrm{Re}\,k} = \sqrt{\kappa} = c_{P2}.$$

Transversal waves: dispersion relation

$$\omega^3 + i\pi\left(\frac{1}{\rho_0^S} + \frac{1}{\rho_0^F}\right)\omega^2 - c_S^2 k^2 \omega - i c_S^2 k^2 \frac{\pi}{\rho_0^F} = 0, \qquad c_S^2 := \frac{\mu^S}{\rho_0^S}.$$

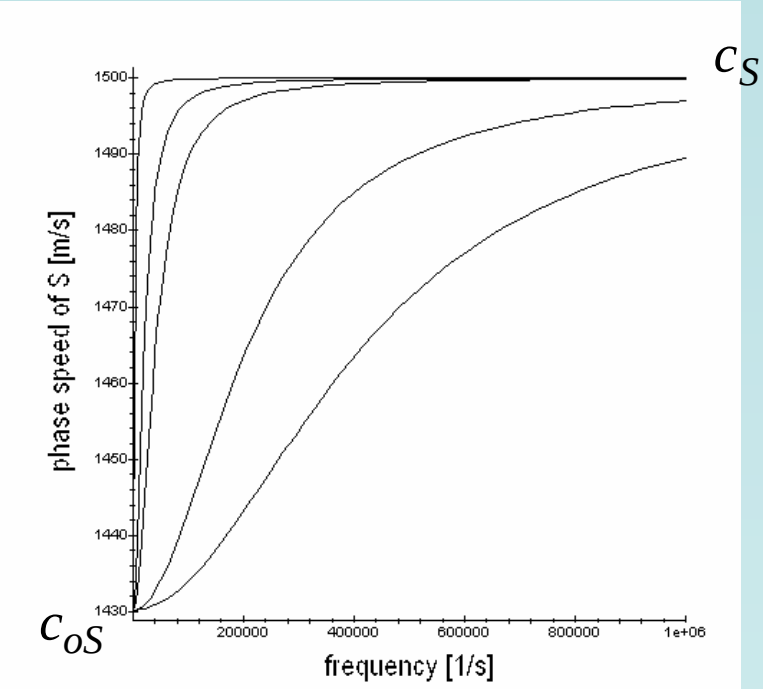

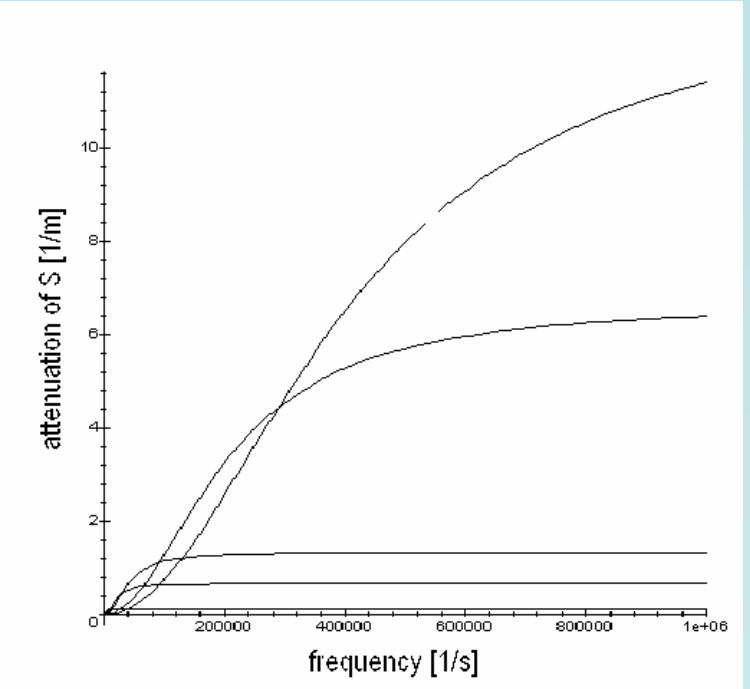

*Phase speed ω/*Re*k and attenuation* Im*k of S-waves. The same data as before.*

Limits:

$$c_{oS} := \lim_{\omega\to 0}\frac{\omega}{\mathrm{Re}k} = \sqrt{\frac{\mu^S}{\rho_0^S + \rho_0^F}}, \qquad \lim_{\omega\to\infty}\frac{\omega}{\mathrm{Re}k} = \sqrt{\frac{\mu^S}{\rho_0^S}} = c_S.$$

Speeds of propagation in Biot‘s model

$$\lim_{\omega\to\infty}\frac{\omega}{\mathrm{Re}k}=\begin{cases}\dfrac{1}{2}\left[\left(c_{P1}^2+c_{P2}^2\right)+\sqrt{\left(c_{P1}^2-c_{P2}^2\right)^2+\dfrac{4Q^2}{\rho_0^S\,\rho_0^F}}\right],\\[2ex] \dfrac{1}{2}\left[\left(c_{P1}^2+c_{P2}^2\right)-\sqrt{\left(c_{P1}^2-c_{P2}^2\right)^2+\dfrac{4Q^2}{\rho_0^S\,\rho_0^F}}\right],\end{cases}$$

$$c_{P1}^2:=\frac{\lambda^S+2\mu^S-\frac{1}{2}Q}{\rho_0^S},$$

$$c_{P2}^2:=\frac{R-\frac{1}{2}Q}{\rho_0^F}.$$

$$\lim_{\omega\to 0}\frac{\omega}{\mathrm{Re}k}=\begin{cases}\sqrt{\dfrac{\lambda^S+2\mu^S+R+Q}{\rho_0^S+\rho_0^F}},\\ 0.\end{cases}$$

Destructive testing, the original soil structure must be damaged, e.g.

- **laboratory testing**
- **acoustic testing from boreholes, for example - explosive**

Cross-hole and down-hole acoustic tests

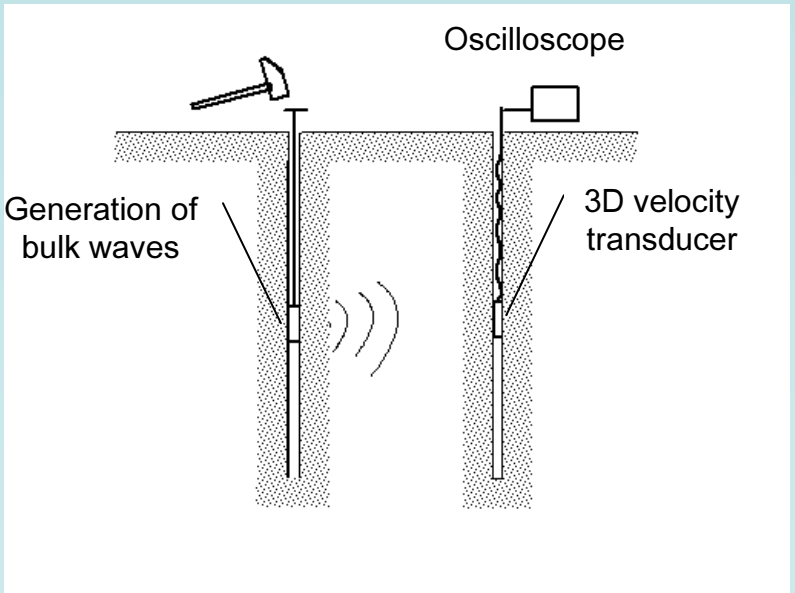

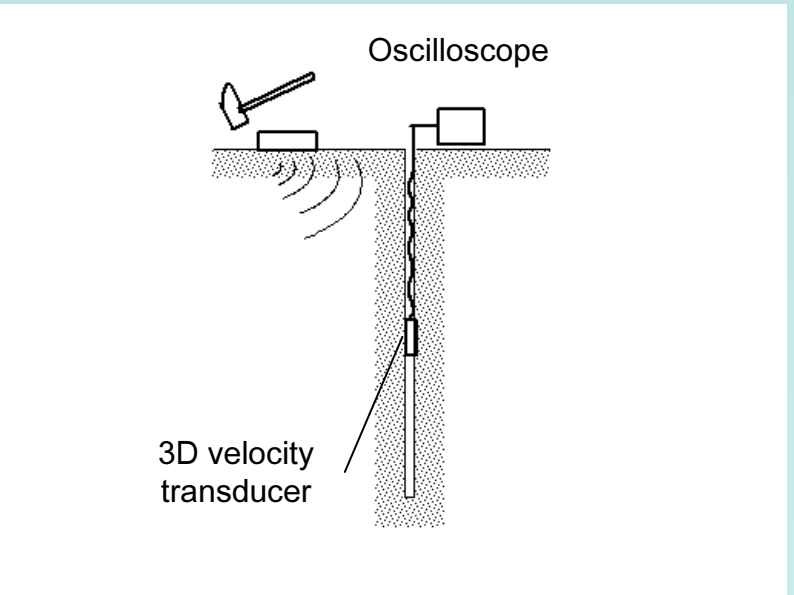

Soil *in situ* Experiments: Cross-Hole Seismic Test (example)

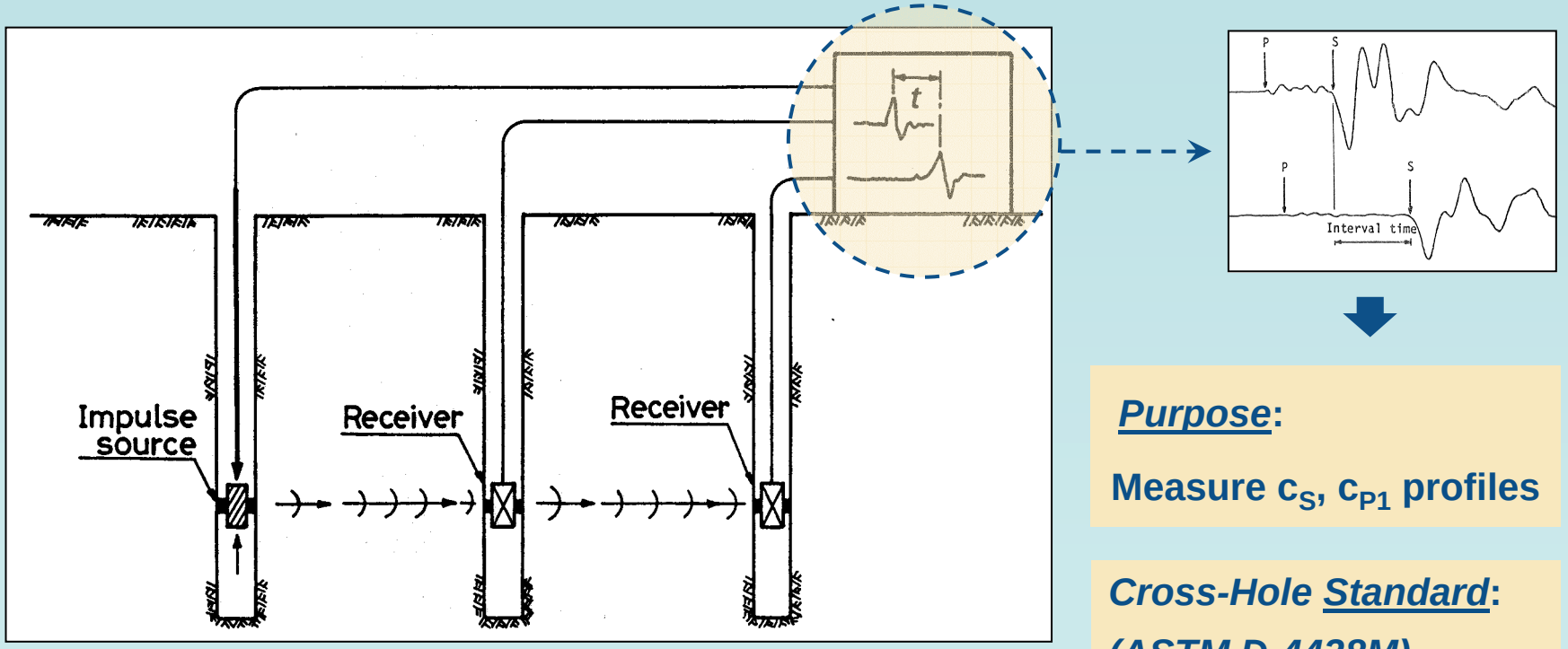

(from Ishihara, 1996)

***Purpose*:**

Measure c_S, c_{P1} profiles

***Cross-Hole Standard*:**

(ASTM D-4428M)

Experimental Measurements of Bulk Waves

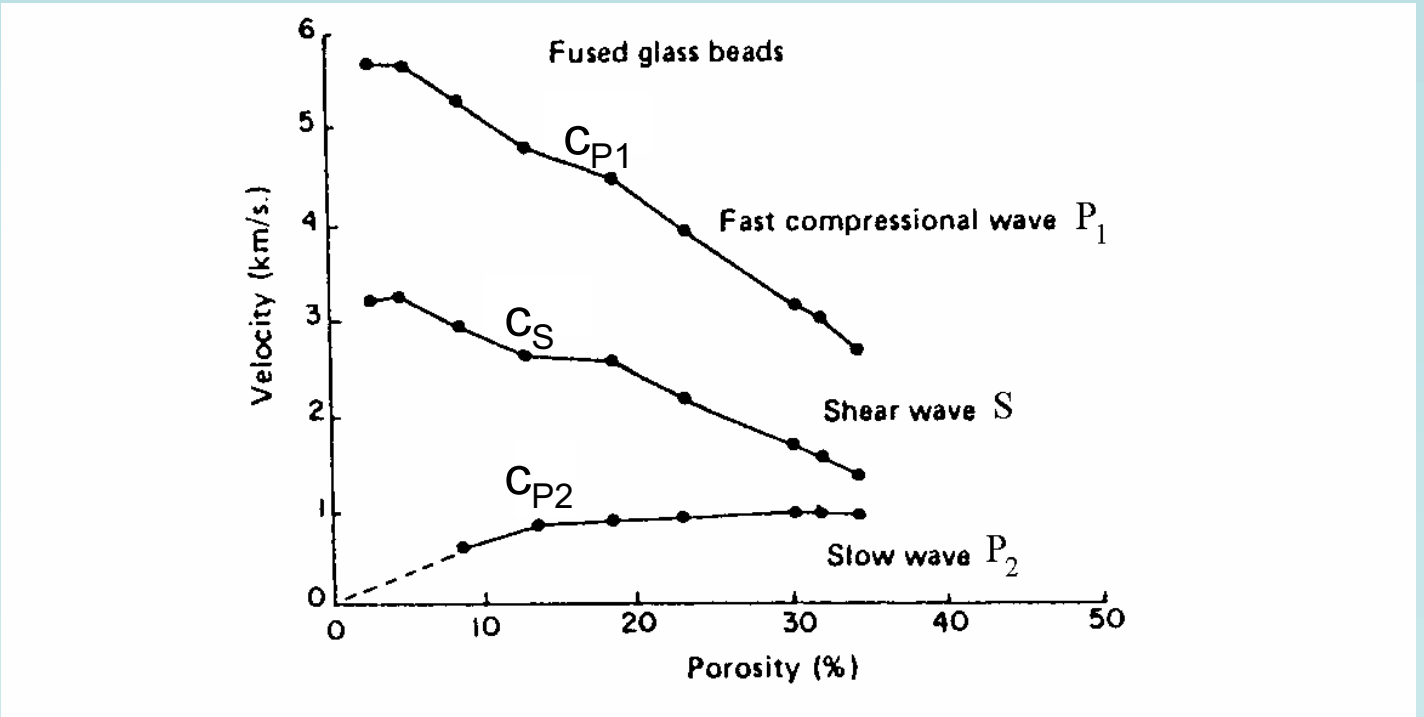

Velocities of bulk waves in an artificial porous material (sintered glass)

T. J. Plona, D. L. Johnson, *Experimental Study of the Two Bulk Compressional Modes in Water-saturated Porous Structures*, Ultrasonic Symp. IEEE, 868-872, 1980.

Experimental Measurements: c_{P1} ,c_S and Porosity Profiles

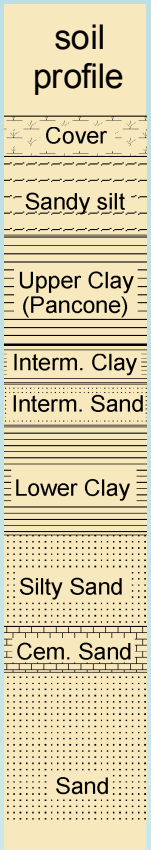

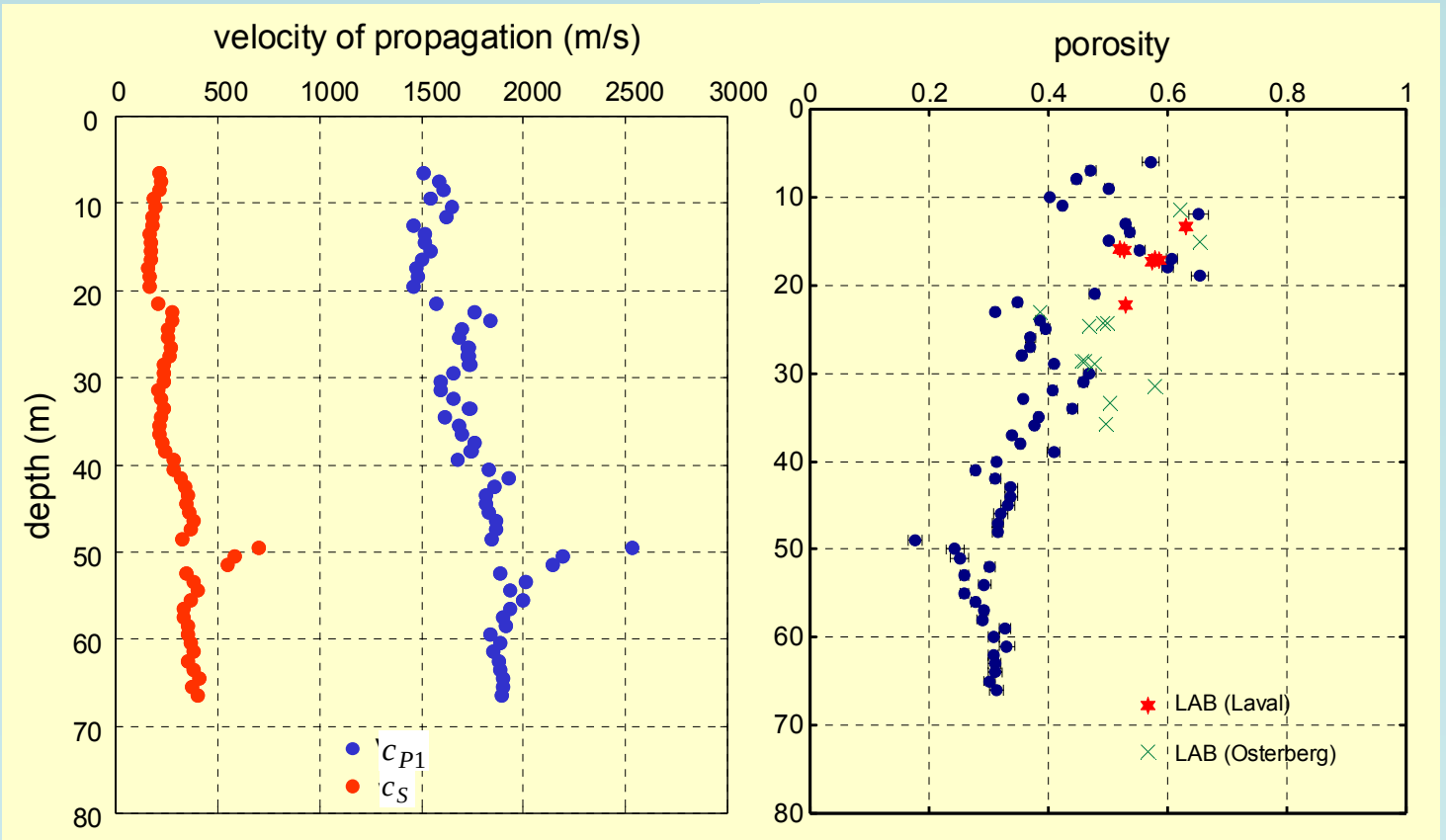

Soil profile and charts of speeds c_{P1} and c_S at Pisa site

Porosity predicted at Pisa site for measured speeds of bulk waves. Comparison with data by Laval and Osterberg laboratory tests

Pisa site.

After: Foti,S., Lai, C., Lancellotta, R.; *Porosity of fluid-saturated porous media from measured seismic wave velocities,* Géotechnique, **52**, 5, 359-373, 2002.
Lai, C.; *Recent Advances in the Solution of Some Parameter-Identification Problems Relevant to Soil Dynamics*, Lecture, Oct. 21, 2002, ROSE School, Pavia, Italy

Surface waves on flat boundaries

- in a half-space of a linear elastic homogeneous material:

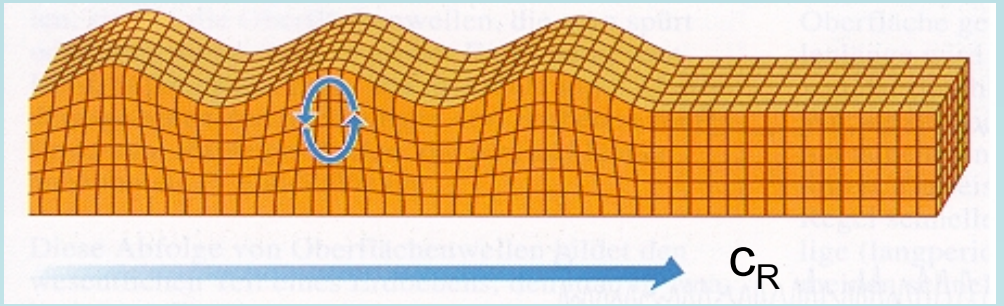

Rayleigh wave

dispersion relation:

$$\left(2-\frac{c_R^2}{c_T^2}\right)^2-4\sqrt{1-\frac{c_R^2}{c_T^2}}\sqrt{1-\frac{c_R^2}{c_L^2}}=0,$$

$$c_L^2 := \frac{\lambda+2\mu}{\rho}, \quad c_T^2 := \frac{\mu}{\rho}.$$

- in a layer over a half-space of a linear elastic homogeneous material:

$$\omega=\frac{c_L}{Hs'}\left[\arctan\left(\frac{\rho c_T^2 s}{\rho' c_T'^2 s'}\right)\right]+n\pi, \quad s^2=1-\frac{c_L^2}{c_T^2}, \quad s'^2=\frac{c_L^2}{c_T'^2}-1.$$

H – thickness of the layer

$c_T > c'_T$ - existence

Example:

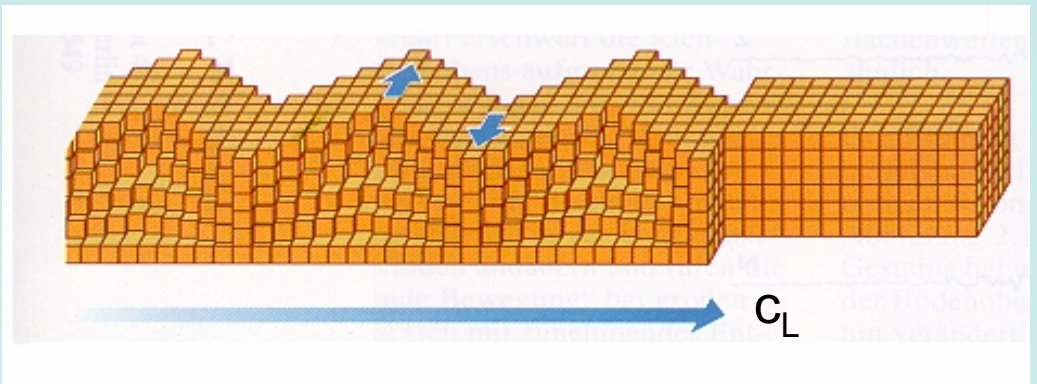

Love wave

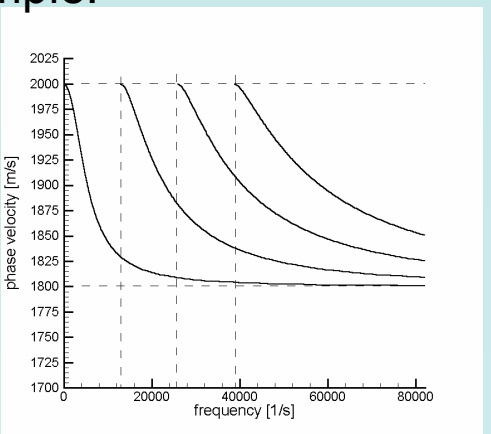

Surface waves within the simple model on the boundary between a porous medium and vacuum*

Potentials for displacements:

$$\mathbf{u}^S = grad\,\varphi^S + rot\,\boldsymbol{\psi}^S, \quad \mathbf{v}^S = \frac{\partial \mathbf{u}^S}{\partial t}, \quad \mathbf{e}^S = sym\,grad\,\mathbf{u}^S,$$

$$\mathbf{u}^F = grad\,\varphi^F + rot\,\boldsymbol{\psi}^F, \quad \mathbf{v}^F = \frac{\partial \mathbf{u}^F}{\partial t}.$$

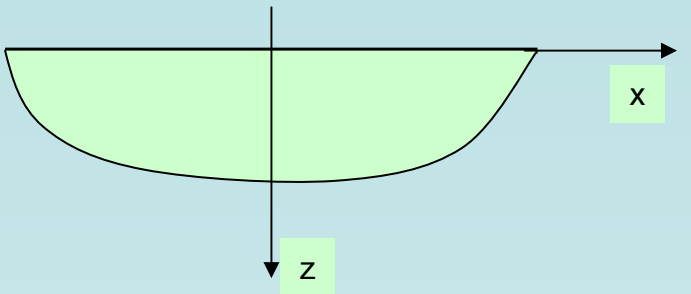

Ansatz for solution:

$$\varphi^S = A^S(z)\mathsf{E}, \quad \varphi^F = A^F(z)\mathsf{E},$$
$$\psi_z^S = B^S(z)\mathsf{E}, \quad \psi_z^F = B^F(z)\mathsf{E},$$
$$\psi_x^S = \psi_y^S = \psi_x^F = \psi_y^F = 0,$$

$$\rho^S - \rho_0^S = A_\rho^S(z)\mathsf{E},$$
$$\rho^F - \rho_0^F = A_\rho^F(z)\mathsf{E},$$
$$n - n_0 = A^\Delta(z)\mathsf{E}.$$

$$\mathsf{E} := e^{i(kx-\omega t)}.$$

Edelman, I., Wilmanski, K.; *Asymptotic analysis of surface waves at vacuum/ porous medium and liquid/porous medium interface*, Cont. Mech. Thermodyn., 25-44, **14**, 1 (2002); and Wilmanski, K., Albers, B.; *Acoustic waves in porous solid – fluid mixtures*, in: *Deformation and Failure of Granular and Porous Continua,* Hutter, K., Kirchner, N. (eds.), Springer, Berlin (2003).

Boundary conditions on the interface vacuum/porous medium:

$$T_{13}\big|_{z=0} = T_{13}^{S}\big|_{z=0} = \mu^{S}\left(\frac{\partial u_1^S}{\partial z} + \frac{\partial u_3^S}{\partial x}\right)\Big|_{z=0} = 0, \qquad \frac{\partial}{\partial t}(u_3^F - u_3^S)\Big|_{z=0} = 0,$$

$$T_{33}\big|_{z=0} = \left(T_{33}^{S} - p^{F}\right)\Big|_{z=0} = c_{P1}^2\rho_0^S\left(\frac{\partial u_1^S}{\partial x} + \frac{\partial u_3^S}{\partial z}\right)\Big|_{z=0} - 2c_S^2\rho_0^S\frac{\partial u_1^S}{\partial x}\Big|_{z=0} - c_{P2}^2\left(\rho^F - \rho_0^F\right)\Big|_{z=0} = 0$$

Substitution of solutions yields a homogeneous set of equations for constants. This yields a dispersion relation determining speeds of propagation of surface waves.

Remark: boundary condition on permeable boundaries:

$$\rho_0^F\frac{\partial}{\partial t}(u_3^F - u_3^S) = \alpha'\left(\frac{p^{F-}}{n^-} - \frac{p^{F+}}{n^+}\right),$$

α‘ – surface permeability; it replaces a surface layer.

High frequency approximation:

$$P_R \sqrt{1-\frac{1}{c_f^2}\left(\frac{\omega}{k}\right)^2} + \frac{r}{c_s^4}\left(\frac{\omega}{k}\right)^4 \sqrt{1-\left(\frac{\omega}{k}\right)^2} = 0,$$

$$P_R := \left(2-\frac{1}{c_s^2}\left(\frac{\omega}{k}\right)^2\right)^2 - 4\sqrt{1-\left(\frac{\omega}{k}\right)^2}\sqrt{1-\frac{1}{c_s^2}\left(\frac{\omega}{k}\right)^2}.$$

Notation

$$c_s := \frac{c_S}{c_{P1}}, \quad c_f := \frac{c_{P2}}{c_{P1}}, \quad r := \frac{\rho_0^F}{\rho_0^S}.$$

For $r=0$ the above relation becomes the Rayleigh dispersion relation.

Otherwise two modes:

- leaky Rayleigh wave with the speed smaller than c_s but larger than c_f,
- Stoneley wave with the speed smaller than c_f.

Low frequency approximation:

Dispersion relation (dimensionless!)

$$\left(\frac{\omega}{k}\right)\left[\left(2-\frac{r+1}{c_s^2}\left(\frac{\omega}{k}\right)^2\right)^2-4\sqrt{1-\frac{r+1}{c_s^2}\left(\frac{\omega}{k}\right)^2}\sqrt{1-\frac{r+1}{rc_f^2+1}\left(\frac{\omega}{k}\right)^2}\right]+O\left(\sqrt{\omega}\right)=0.$$

Hence we obtain two solutions (physical units!):

- Stoneley wave whose speed of propagation is of the order $O\left(\sqrt{\omega}\right)$
- Rayleigh wave whose speed of propagation follows from the equation:

$$\left(2-\frac{c_{P1}^2}{c_{oS}^2}\left(\frac{\omega}{k}\right)^2\right)^2-4\sqrt{1-\frac{c_{P1}^2}{c_{oS}^2}\left(\frac{\omega}{k}\right)^2}\sqrt{1-\frac{c_{P1}^2}{c_{oP1}^2}\left(\frac{\omega}{k}\right)^2}=0.$$

Nondestructive testing: surface waves, the original structure of the soil is not influenced, e.g. SASW (Spectral Analysis of Surface Waves); different configurations possible (e.g. multistations)

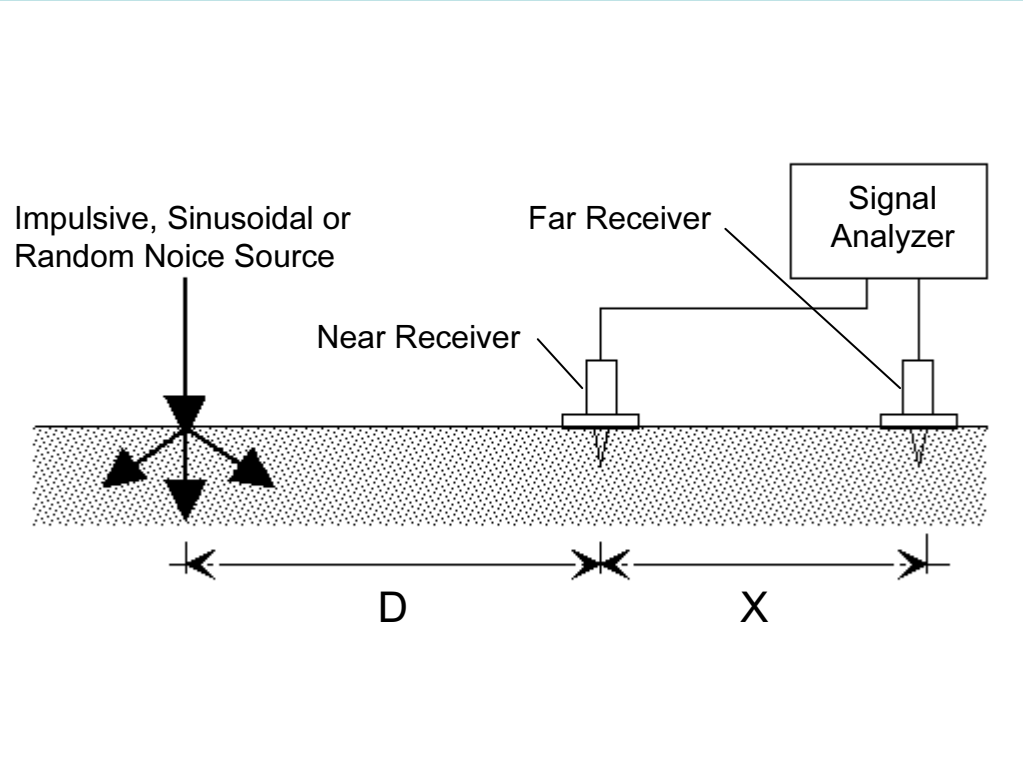

Nondestructive testing of soils

Experimental Measurements: *Instrumentation*

Dropped weight as a seismic source

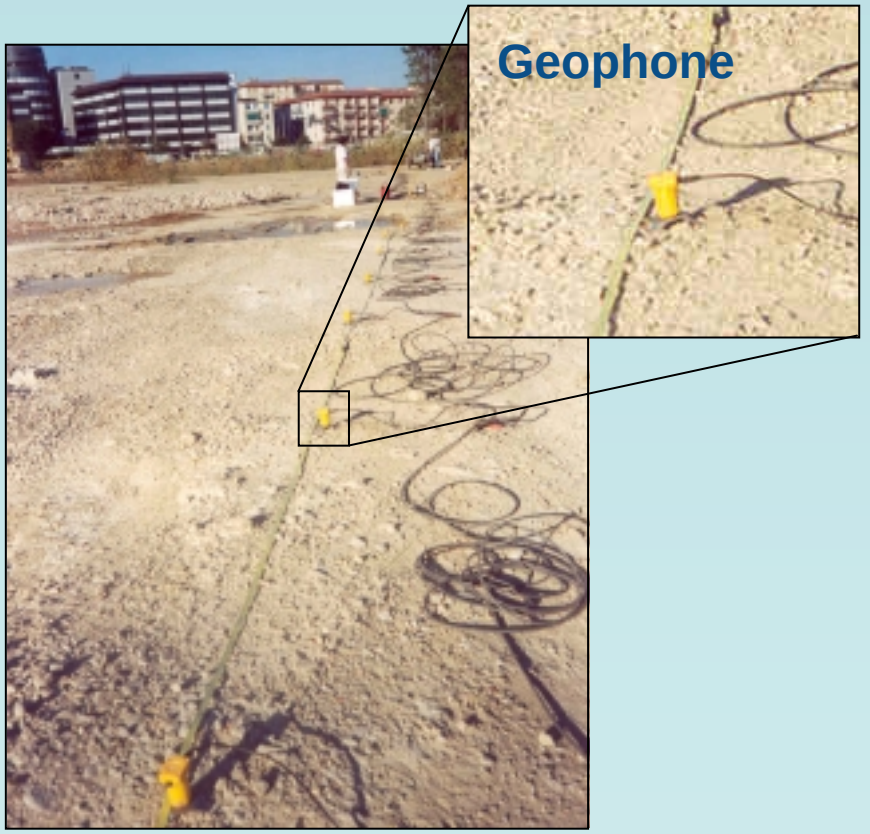

Linear array of geophones

Final remarks

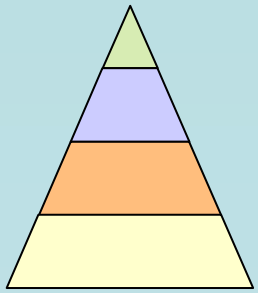

1) Results of wave analysis should be extended on heterogeneous and stratified media. In particular – existence of additional modes.

2) A model of unsaturated poroelastic materials should be developed in which a coupling of phase transformation (evaporation/condensation) with acoustic waves should be incorporated.

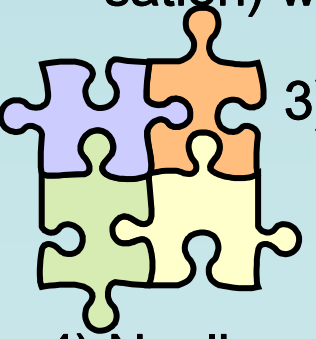

3) A selfconsistent method of micro-macro-transition must be developed in order to avoid large discrepancies between geometrically and dynamically consistent models.

4) Nonlinear effects such as a dependence on equilibrium porosity or on confining pressure in granular materials must be included in the wave analysis. This leads inevitably to nonlinear waves (e.g. soliton-like or nonlinear surface waves).

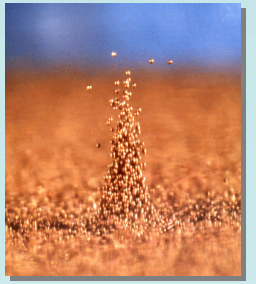

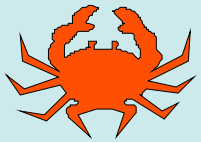

5) As estimations of porosity are an inverse problem they require a mathematical analysis of solutions which is entirely missing.